

Dielectric Variation In Paper and Its Effects On Electrophotographic Printing

Nikolas Provas^{1,2,3}, Andrew Cassidy² and Mituo Inoue³

¹Department of Materials Science and Engineering, McMaster University, Hamilton, Ontario, Canada

²McGill University, Montreal Quebec, Canada

³PAPRICAN, Pointe-Claire, Quebec, Canada

Abstract

Print density mottle of the solid black images in electrophotographic printing is related to paper structure. We found that mottle in commercial papers has a strong correlation with PCC filler distribution, but a very weak correlation with the overall visual formation. We explain these observations using a new mathematical model that simulates the electrostatics of toner transfer. Simulations show that print density mottle is strongly influenced by spatial variations in the dielectric permittivity of paper and paper thickness variations. It is shown that the permittivity is strongly influenced by filler distribution and to a lesser extent by visual formation.

Introduction

Electrophotographic printing¹⁻³ (e.g., Xerography) has recently become a commercially viable alternative to conventional printing in the area of short-run color printing. Relatively little is known, however, about how this process is influenced by the properties of the paper substrate. Paper's heterogeneous spatial structure and its even more complex interactions with the electrostatics of the photoreceptor make the prediction of print quality in electrophotography very difficult.

One of the emerging print quality issues associated with electrophotography is severe print mottle in solid images, particularly in color printing. Even for simple monochrome black printing, print density mottle is still clearly visible. Since toner penetrates very little into the paper, even after thermal fusing, print density mottle or toner thickness variation is primarily caused by uneven toner deposition onto the paper.

In electrophotography, printing occurs when charged toner particles are *electrostatically* transferred from a photoreceptor plate onto the paper surface under the action of an electric field. Paper has often been treated as a uniform layer in designing the electrophotographic printing processes.¹⁻³ In practice, however, paper is quite non-

uniform and non-homogeneous.^{4,5} This can give rise to print density mottle through variations in (a) mass density (b) paper thickness (c) moisture and (d) surface topography. While mass density and moisture have been shown to change the *overall* dielectric constant of paper,⁶ their point-to-point variations can also lead to print density mottle through variations in toner transfer forces.⁷ In this paper we discuss experiments and numerical simulations showing how spatial variations in paper (fillers, formation, thickness variations) influence the uniformity of electrostatic transfer and, ultimately print density mottle.

Analysis of Print Density Variations

Methods and Materials:

Experiments were performed on 5 commercial paper samples as well as standard handsheets. In commercial samples, the formation and filler distributions were analyzed. In the handsheets, only formation was examined, as they did not contain filler. The main source of filler in the commercial sheets was PCC. All papers were printed at 100% (solid black) toner coverage on a Xerox 5090 copier.

Formation and print density were measured on 20 mm x 20 mm zones. To relate paper structures to print density variations in the same region of the paper, print density and formation were measured on the same zones. As filler measurements were destructive, they were made on zones of the same size on sample sheets different from those printed. Statistical fluctuations in data were minimized by averaging measurements of all quantities over several zones per sheet and several sheets per sample (a total of 30 zones for print density and filler and 10 for print density distributions).

Measurements of formation, filler and print density were made using the Paprican microscanner device.⁸ This device determines optical formation by measuring the variation of intensity of white light *transmitted* through a paper sheet. Print density was measured with the same device using light *reflected* from printed samples. The *burnout* method was used to reveal filler distributions near the paper surface.⁹ Light reflected from the burned-out

paper surface thus gives a reasonable indication of the filler distribution. The spatial resolution of the microscanner is approximately $120\mu\text{m} \times 160\mu\text{m}$.

All PCC-filled commercial samples printed as described above *always* exhibited characteristic print density variations on length scales up to about 1-2mm. This mottle feature size was not, however, present in handsheet data of this investigation.

Spatial distributions of formation, filler and print density were analyzed using the *two-point density-density correlation*, defined as

$$G(x,y) = \left\langle (m(i,j) - \langle m \rangle)(m(i+x, j+y) - \langle m \rangle) \right\rangle \quad (1)$$

where $m(i,j)$ represents either formation, filler or print density fields. The indices i,j discrete pixels in data zones. The variables x,y are also discrete, and are defined over the same range. The quantity $\langle m \rangle$ denotes the mean value of the field in the area of a zone. Angled brackets imply that the product in Eq. (1) is spatially averaged over all points (i,j) in the zone (using periodic boundary conditions), and over all zones in a sample type. As paper is not isotropic, $G(x,0) \neq G(0,y)$. In all our formation measurements there was visible anisotropy. This was also present in the other measurements as well, although less apparent. Its origin in commercial sheets can be traced to the anisotropic fiber orientation. The correlation function was normalized by dividing it by the covariance of the corresponding field (i.e., $G(0) = 1$).

Commercial Filled Sheets:

Figures 1a-c show $G(r)$ for the *print density*, *filler distribution* and *formation* corresponding to one of the commercial samples in the study ($75\text{g}/\text{m}^2$, 14% filler). Machine and cross directions are indicated. Data of $G(r)$ for all commercial samples was similar in trend to that shown here. The structure in the print density correlation function (Fig. 1a) predicts a visually distinct contrast in print density between structures on the scale $r_1 \approx 650\mu\text{m}$ and the characteristic space between them $d \approx 0.55\mu\text{m}$ (CD) ($r_1 \approx 900\mu\text{m}$, $d \approx 1.1\mu\text{m}$ in MD). The correlation function of the filler distribution (Fig. 1b) in the commercial sheets predicts spatial structure for the fillers commensurate to that of print density. The correlation function of the optical formation of the commercial sheets (Fig. 1c) predicts floc sizes greater than 5mm, and bears little resemblance to the correlation functions of print density and filler distributions on the scale of ~ 1 -2mm. (The decay of the correlation to a non-zero value at large distances is a *finite-size* effect, artifact of the small size of the sampling zone relative to the typical floc size).

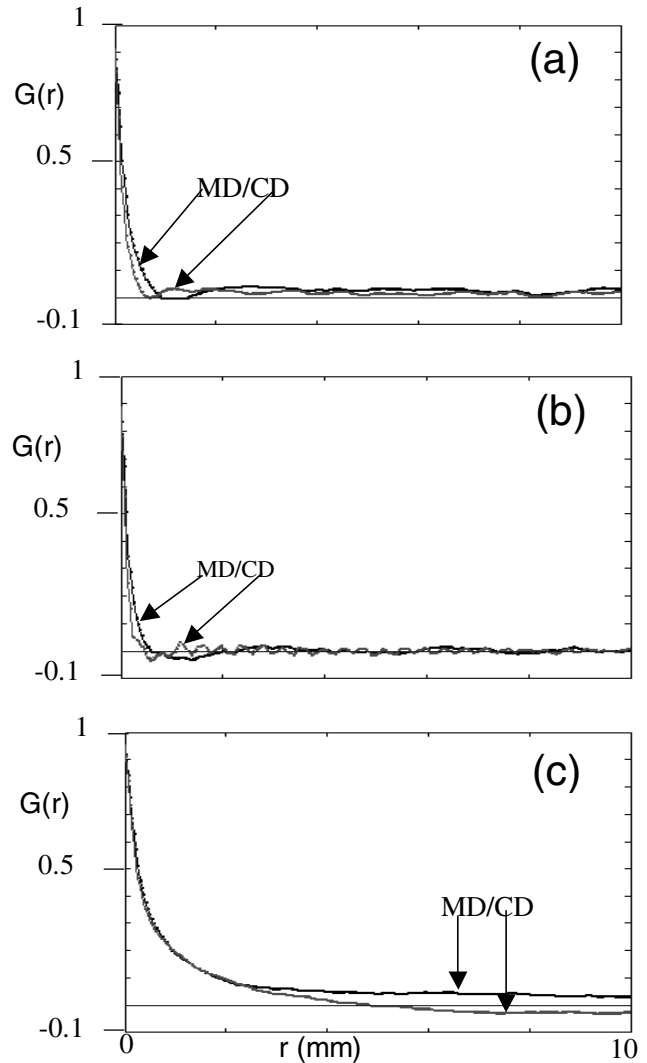


Figure 1. Two-point correlation function of (a) print density, (b) filler and (c) formation of commercial PPC-filled sheets

Handsheets:

Figures 2a-b show plots of $G(r)$ for *print density* and *formation* in handsheets along the x and y directions. The print density correlation function predicts a uniform appearance of print density on scales 5-10mm (consistent with visual observation), with very *weak* features on scales around 1mm, in contrast to the PCC-filled commercial samples. The formation $G(r)$ also displays large finite-size effects, another indication of large flocs on the order of 5-10mm.

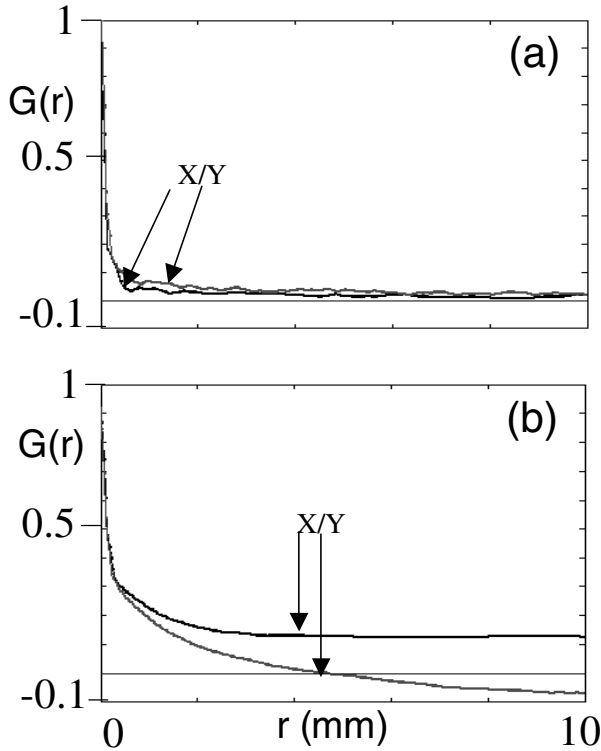


Figure 2. Two-point correlation function of (a) print density and (b) formation of handsheets

Discussion:

The transfer of toners to paper occurs by a local electrostatic field created between the photoreceptor and toner layers. As the electric field must act *through* the paper, it is strengthened or weakened in proportion to the local dielectric constant of the paper. The local dielectric constant of the paper depends on the density and volume fractions of the constituents within the paper.⁷ (Other factors not considered here, and influencing the toner transfer force are local paper thickness (see below), roughness and moisture content). In the case of commercial filled sheets, the larger dielectric constant of PCC filler over that of cellulose suggests that filler-rich regions of filler should be strongly correlated to regions of print density variation. This is a plausible reason for the similar length scale of features in the toner and filler densities at the 1-2mm scale. In the case of handsheets, the local dielectric constant can only depend on formation. The finite size effect of Fig. 2(b) precludes us from making a conclusive link between visual formation and print density in hand sheets.

Modeling Toner Transfer

We recently reported on a model that simulates toner transfer forces in electrophotography. The model divides the paper into numerically small discrete elements e^j , the surface of each carrying a charge density σ^j . Toner forces at

each point in the toner layer are computed by integrating the force fields due to all charged elements. The basic input into the model is an approximation of the *local* corona charge field of the paper, given by

$$\sigma^j = \frac{V}{h_d \left[1 - \left(\frac{\langle \epsilon_p^j \rangle - 1}{\langle \epsilon_p^j \rangle} \right) \frac{\langle h_p^j \rangle}{h_d} \right]} \quad (2)$$

where V is the applied machine voltage, $\langle h_p^j \rangle$ is the average *local* paper thickness over an element, h_d is the thickness of the printing gap, and $\langle \epsilon_p^j \rangle$ is the *local, effective*, dielectric constant defined throughout the volume of an element. It is approximated by the theory of binary mixtures.⁶

The charge density σ^j provides the force field necessary for toner transfer. Inspection of Eq. (2) shows that the strength of this field depends on two main paper factors: *local dielectric constant* of the paper $\langle \epsilon_p^j \rangle$ and *local paper thickness*.

Figure 3a shows a gray-scale surface of a simulated paper (produced by a 3D fiber-network model of paper). Lighter/darker pixels denote lower/higher heights, respectively. The x and y axes are in units of 5 μ m (similarly for Figs. 3b-c). The simulated paper comprised 89% fibers (by mass), from a Poisson length distribution with mean length \approx 1.5mm, and 11% Poisson-distributed filler agglomerates of mean size of 10 μ m. Figure 3b shows the corresponding map of the x-y filler distribution. Lighter colors represent higher filler concentrations. The white rectangular box shown in Figs. 3a-b represents an area within which the toner transfer model was used to compute the transfer forces (Fig. 3c) on a uniform layer of toner representing a solid print. Dark/light pixels denote high/low toner transfer forces. Force is in units of 0.5 μ N, $V = 5$ kV and $h_d = 25\mu$ m. Toners were treated as spherical particles with a radius 5 μ m and charge 5×10^{-15} C. Figures 3b-c show a clear spatial correlation between higher toner transfer forces and filler-rich regions, as seen experimentally. The effects of paper thickness variations have also been examined using a model that directly solves Poisson equations. Results will be presented in an upcoming publication.

References

1. J. Johnson, "Principles of Non-impact Printing", Palatino Press, Irvine, USA (1992).
2. R. M. Schaffert, "Electrophotography", Focal Press, New York (1975).
3. R. B. Comizzoli, G.S. Lozier and D.A. Ross, "Electrophotography -A Review", *RCA Review*, **33**, 406 (1972).
4. B. Norman and D. Wahren, *Svensk. Papperstidn.*, **77**(11), 362 (1974).

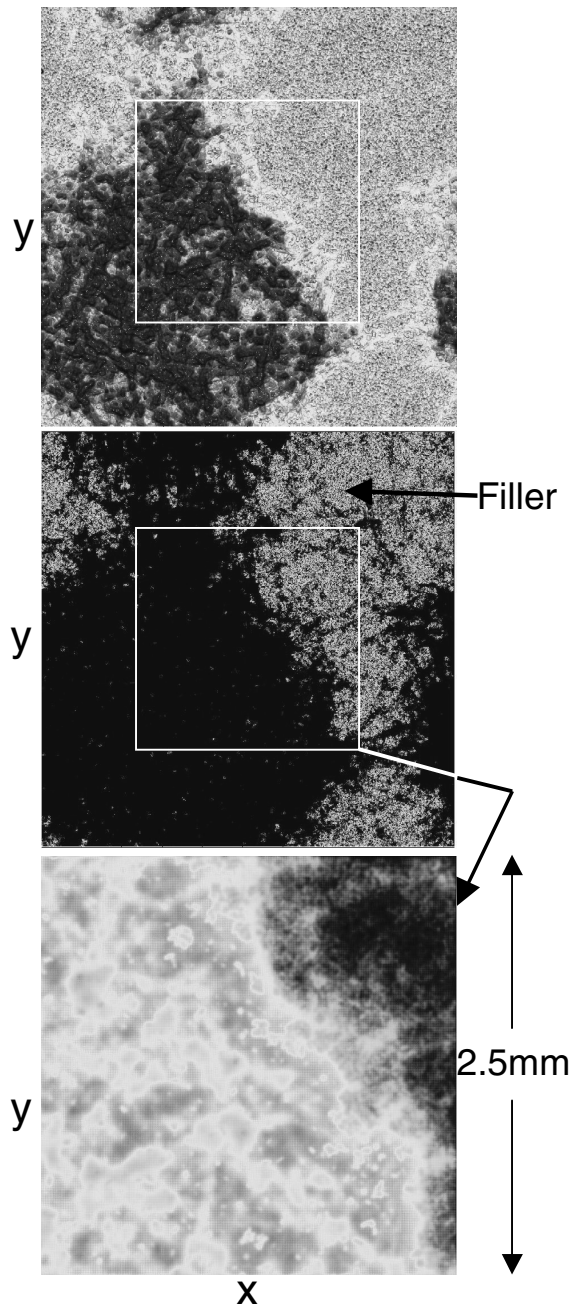


Figure 3. (a) Surface profile of simulated filled paper (b) filler distribution, (c) force map on toner layer.

5. H. Corte and O.J. Kallmes, "Statistical Geometry of a Fibrous Network", in *Formation and Structure of Paper*, (edited by F. Bolam), British Paper and Board Makers Assoc., London (1962).
6. S. Simula, S. Ikalainen, K. Niskanen, T. Varpula, H. Seppa and A. Paukku, *J. Imag. Sci. and Tech.* **43**(5), 472 (1999).
7. M.-K. Tse, D.J. Forrest and F.Y. Wong, *IS&T NIP 15: International Conference on Digital Printing Technologies*, 486 (1999).
8. R. J. Trepanier, *Tappi J.*, **72**(12), 153 (1989).
9. M. O'Neill and B. Jordan, *JPPS*, **26**(4), 131 (2000).

Biography

Nikolas Provatas received his Doctorate in Theoretical Physics from McGill University in 1994. He worked at the Physics Department of the University of Helsinki between 1994-1996. From 1996-1999 he was a Research Associate at the University of Illinois at Urbana-Champaign. His research subjects include paper physics, solidification of metals and combustion theory. In 1999 he joined the Pulp and Paper Research Institute of Canada, where he has been applying mathematical modeling of paper structure to the design of improved printing paper.